



A Passive Method for the Detection of Explosives and Weapons-Grade Plutonium in Nuclear Warheads

Huang Meng^a, Zhu Jianyu^b, Wu Jun^b, and Li Rui^c

^aInstitute of Applied Physics and Computational Mathematics, Beijing, China; ^bCenter for Strategic Studies, China Academy of Engineering Physics, Beijing, China; ^cSoftware Center for High Performance Numerical Simulation, China Academy of Engineering Physics, Beijing, China

ABSTRACT



Before a nuclear warhead is dismantled, the special nuclear material and explosives must be identified and authenticated. This paper proposes a passive method to detect and identify weapons-grade plutonium cores and explosives in nuclear warheads based on neutron analyses techniques. This paper first describes the principles of a passive detection method that calculates the element number ratio (namely the ratio between the nucleus numbers of two different elements) of the element of interest to identify a source and how this method could be applied to the detection of warhead explosives. Second, a simulation of weapons-grade plutonium using JMCT software is described. The simulation assumes the elemental components of the explosives are activated by the production and transport of neutrons from the weapons-grade plutonium core and counted the gamma ray emissions of from the resultant hydrogen, carbon, and nitrogen nuclides with a high-purity germanium detector (HPGe) array. After an hour of counting, the element number ratios of these elements in the simulation were reconstructed and accurately matched the values for the explosives in the warhead. These results suggest that the passive method can be used to identify the presence of weapons-grade plutonium in the warhead. In addition, the simulation showed that the passive method can also discriminate between the various types of explosives in warheads, providing important physical information for the verification process during dismantlement.

ARTICLE HISTORY

Received 19 October 2017
Accepted 26 June 2018

Introduction

Future global nuclear disarmament may require the dismantlement of nuclear warheads. The dismantlement and disarmament of the nuclear warhead requires the separation of the special nuclear material and the explosive.¹ There is always a risk that a verified party may use deceptive methods to avoid the obligations of nuclear disarmament and substitute

CONTACT Huang Meng  hm.max@126.com  Institute of Applied Physics and Computational Mathematics, Beijing 100094, China.

Color versions of one or more of the figures in the article can be found online at www.tandfonline.com/gsgs.

© 2018 Taylor & Francis Group, LLC

fake warheads for real ones. Due to the complexities and difficulties of shaping explosives to fit the warhead shell, these fake warheads may not contain explosives. Therefore, the presence of the special nuclear material and the explosive should be confirmed by the inspectors to ensure that the nuclear warhead contains both components before the warhead is dismantled.

There are two methods to detect warhead explosives using neutron analysis: “active methods” and “passive methods.” In both methods, elements within the explosive are irradiated by neutrons and the resultant neutron induced γ rays from the explosive nuclides are counted.² The source of those neutrons differs for each method. The active method uses an external neutron source to irradiate the explosive in the warhead. The passive method relies on neutrons that originate in the weapons-grade plutonium (WgPu) core. The passive method is likely to be easier to execute in the field because it uses simple measurement equipment and does not require an external source of neutrons, thus increasing its agility.

The passive method can be summarized in three steps: First, (n,γ) reactions occur between the neutrons produced by the warhead and the elements in the explosive, resulting in characteristic γ rays. Second, by characterizing the γ rays, the elements of the explosive can be detected and recognized. Finally, by analyzing the strengths of these γ rays, the element constitution and the type of the explosive may be calculated.

This paper describes principles of the passive method, evaluates its feasibility, and presents the results of a simulated case.

Principles of passive method

The fissile material (such as WgPu and depleted uranium) in the WgPu warhead splits spontaneously and produces fission neutrons, resulting in neutron irradiation in the warhead. When the neutrons enter the explosive they have (n,γ) reactions with the elements in the explosive, and characteristic γ rays of those elements are produced. By detecting the characteristic γ rays, the elements of the explosive in the warhead may be detected and identified.

By analyzing the strengths of the characteristic γ rays of hydrogen, carbon, nitrogen, and oxygen, the element number ratios (namely the ratio between the nucleus numbers of two different elements), such as hydrogen-nitrogen ($[H]/[N]$), carbon-nitrogen ($[C]/[N]$), and oxygen-nitrogen ($[O]/[N]$) number ratios, can be calculated. It should be noted that, since the abundances of hydrogen-1, carbon-12, nitrogen-14, and oxygen-16 are constant in the explosive (99.99%, 98.93%, 99.63%, and 99.76% respectively), the element number ratios of hydrogen, carbon, nitrogen, and oxygen can

be calculated according to the ratios of the numbers of hydrogen-1, carbon-12, nitrogen-14, and oxygen-16. It is assumed in the simulation that hydrogen-1, carbon-12, nitrogen-14, and oxygen-16 occupy 100% of the nuclei of each element. Since the microscopic cross-section of the (n,γ) reaction of oxygen-16 is very small, and far less than those of hydrogen-1, carbon-12, and nitrogen-14, the detection of oxygen-16 is not discussed here. Table 1 shows the energy and branch ratios of the characteristic γ rays of the (n,γ) reactions of hydrogen-1, carbon-12, and nitrogen-14, and the calculation of [H]/[N] and [C]/[N].³ Next, the calculation method of [H]/[N] and [C]/[N] will be introduced.

The number of the characteristic γ rays with energy of E_γ produced by the (n,γ) reactions between the nuclide A of the explosive in the warhead and the neutron per unit time ($S_A(E_\gamma)$) has a relationship with the microscopic cross-section of the (n,γ) reaction, the branch ratio of the characteristic γ rays with the energy of E_γ , the neutron flux density, and the nucleus density of the nuclide A. It can be expressed as:

$$S_A(E_\gamma) = \int_V n_A(\vec{r}) \cdot f_A(E_\gamma) \cdot dV$$

$$n_A(\vec{r}) = \int N_A \cdot \sigma_A(E_n) \cdot \phi(\vec{r}, E_n) \cdot dE_n \quad (1)$$

where $n_A(\vec{r})$ is the spatial density of the (n,γ) reactions between the nuclide A and the neutrons per unit time at the position of \vec{r}

$f_A(E_\gamma)$ is the branch ratio of the characteristic γ ray with the energy of E_γ
 N_A is the nucleus density of the nuclide A, E_n is the neutron energy
 $\sigma_A(E_n)$ is the microscopic cross-section of the (n,γ) reaction between the neutron with energy of E_n the nuclide A
 $\phi(\vec{r}, E_n)$ is the neutron flux density at the position of \vec{r}

After the production of the characteristic γ ray of the nuclide A, it would likely emit from the warhead with some probability. The number of the

Table 1. Characteristic γ rays of (n,γ) reactions of hydrogen-1, carbon-12 and nitrogen-14.

Nuclide	Energy of γ ray (MeV)	Branch ratio (%)
Hydrogen-1	2.22	100
Carbon-12	4.95	68
Nitrogen-14	1.88	18.78
Nitrogen-14	3.68	14.53
Nitrogen-14	4.51	16.72
Nitrogen-14	5.27	29.88
Nitrogen-14	6.32	18.24
Nitrogen-14	10.83	14.33

characteristic γ rays with the energy of E_γ emitted from the warhead per unit time ($K_A(E_\gamma)$) can be expressed as:

$$K_A(E_\gamma) = \int_V n_A(\vec{r}) \cdot f_A(E_\gamma) \cdot P(\vec{r}, E_\gamma) \cdot dV \quad (2)$$

where $P(\vec{r}, E_\gamma)$ is the average probability that the characteristic γ rays with the energy of E_γ produced at the position of \vec{r} emit from the warhead.

When simulating $n_A(\vec{r})$, it is found that, since the microscopic cross-sections of the (n, γ) reaction between the neutrons with low energy (below 1 eV) and hydrogen-1, carbon-12, and nitrogen-14 are much higher than those of middle-energy neutrons and fast neutrons for each nuclide, and the neutrons with low energy (below 1 eV) account for more than 20% of the neutrons entering the explosive in the warhead, only the (n, γ) reactions between the neutrons with low energy and the explosive nuclides are taken into account in the calculation of $n_A(\vec{r})$. Taking hydrogen-1 for example, the microscopic cross-section of the (n, γ) reaction between the thermal neutron with energy of 0.025eV and hydrogen-1 is two orders of magnitude higher than that of the neutron with energy of 1 keV, and four orders of magnitude higher than that of the neutron with energy of 1 MeV. Based on the ENDF/B-VI database,⁴ the microscopic cross-sections of (n, γ) reactions of hydrogen-1, carbon-12 and nitrogen-14 are in the pure $1/v$ regime (v is the neutron velocity) in the energy range of $0 \sim 1\text{eV}$, $\frac{\sigma_{H-1}(E_n)}{\sigma_{N-14}(E_n)}$ and $\frac{\sigma_{C-12}(E_n)}{\sigma_{N-14}(E_n)}$ are almost constant (below 1 eV), and their values are about 4.43 and 4.53×10^{-2} respectively (these values are named $\left[\frac{\sigma_{H-1}(E_n)}{\sigma_{N-14}(E_n)}\right]_T$ and $\left[\frac{\sigma_{C-12}(E_n)}{\sigma_{N-14}(E_n)}\right]_T$ respectively), and the relative standard deviation of each term is well below 1% (see Figure 1). Based on this analysis, the formula for $n_A(\vec{r})$ of hydrogen-1 and carbon-12 can be simplified. Taking hydrogen-1 for example, the formula of $n_{H-1}(\vec{r})$ can be rewritten as:

$$n_{H-1}(\vec{r}) = \frac{N_{H-1}}{N_{N-14}} \cdot \left[\frac{\sigma_{H-1}(E_n)}{\sigma_{N-14}(E_n)}\right]_T \cdot n_{N-14}(\vec{r}) \quad (3)$$

Furthermore, the formula for the number ratio between the characteristic γ rays of hydrogen-1 and nitrogen-14 emitted from the warhead ($\frac{K_{H-1}(E_{\gamma 1})}{K_{N-14}(E_{\gamma 2})}$) can be calculated:

$$\frac{K_{H-1}(E_{\gamma 1})}{K_{N-14}(E_{\gamma 2})} = \frac{N_{H-1}}{N_{N-14}} \cdot \left[\frac{\sigma_{H-1}(E_n)}{\sigma_{N-14}(E_n)}\right]_T \cdot \frac{f_{H-1}(E_{\gamma 1})}{f_{N-14}(E_{\gamma 2})} \cdot \frac{\int_V n_{N-14}(\vec{r}) \cdot P(\vec{r}, E_{\gamma 1}) \cdot dV}{\int_V n_{N-14}(\vec{r}) \cdot P(\vec{r}, E_{\gamma 2}) \cdot dV} \quad (4)$$

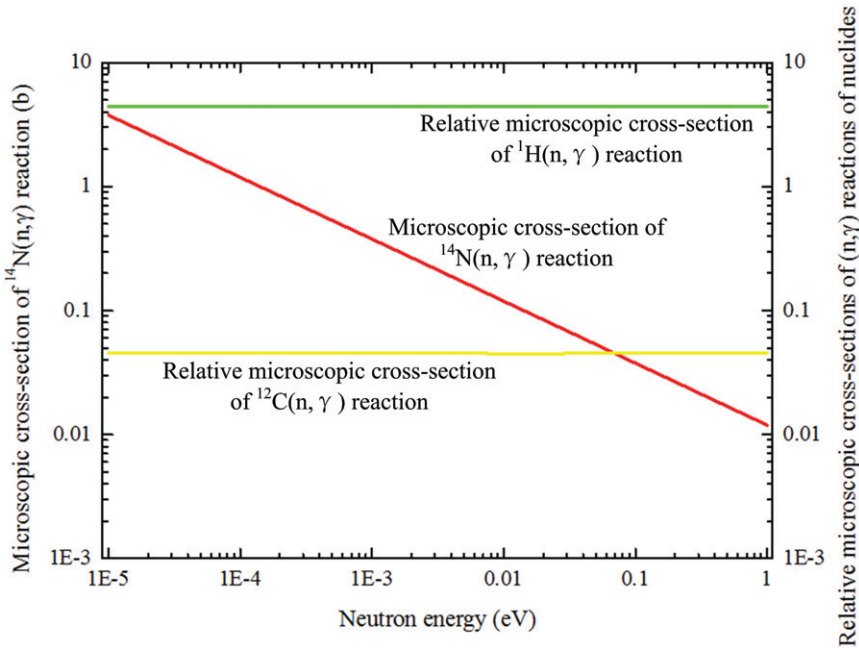


Figure 1. Microscopic cross-sections of (n,γ) reactions of hydrogen-1, carbon-12 and nitrogen-14.

where $E_{\gamma 1}$ and $E_{\gamma 2}$ are the energy of the characteristic γ rays of hydrogen-1 and nitrogen-14 respectively. Then, the element number ratio between hydrogen and nitrogen ($[H]/[N]$) of the explosive can be calculated:

$$[H]/[N] = \frac{N_{H-1}}{N_{N-14}} \cdot \frac{A_{N-14}}{A_{H-1}} = \frac{\frac{K_{H-1}(E_{\gamma 1})}{K_{N-14}(E_{\gamma 2})} \cdot \frac{A_{N-14}}{A_{H-1}}}{\left[\frac{\sigma_{H-1}(E_n)}{\sigma_{N-14}(E_n)} \right]_T \cdot \frac{f_{H-1}(E_{\gamma 1})}{f_{N-14}(E_{\gamma 2})} \cdot \frac{\int_V n_{N-14}(\vec{r}) \cdot P(\vec{r}, E_{\gamma 1}) \cdot dV}{\int_V n_{N-14}(\vec{r}) \cdot P(\vec{r}, E_{\gamma 2}) \cdot dV}} \quad (5)$$

where A_{H-1} and A_{N-14} are the abundances of hydrogen-1 and nitrogen-14 respectively. Similarly, $[C]/[N]$ and $[O]/[N]$ can be also calculated.

In Eq 5, $\int_V n_{N-14}(\vec{r}) \cdot P(\vec{r}, E_{\gamma}) \cdot dV$ is the absorption efficiency of the warhead to the γ ray. If the radial profiles of the γ emissions from the different nuclei are the same, which is justified by the identical energy dependence of (n,γ) cross-sections for the different nuclei, the absorption efficiency only depends on the energy of the γ ray. Using $C(E_{\gamma})$ to mark the absorption efficiency, the absorption efficiency can be expressed by the following, per Equation 2:

$$C(E_{\gamma}) = \int_V n_{N-14}(\vec{r}) \cdot P(\vec{r}, E_{\gamma}) \cdot dV = \frac{K_{N-14}(E_{\gamma})}{f_{N-14}(E_{\gamma})} \quad (6)$$

Therefore, by measuring the strengths of the various characteristic γ rays of nitrogen-14 emitted from the warhead and calculating the ratios between

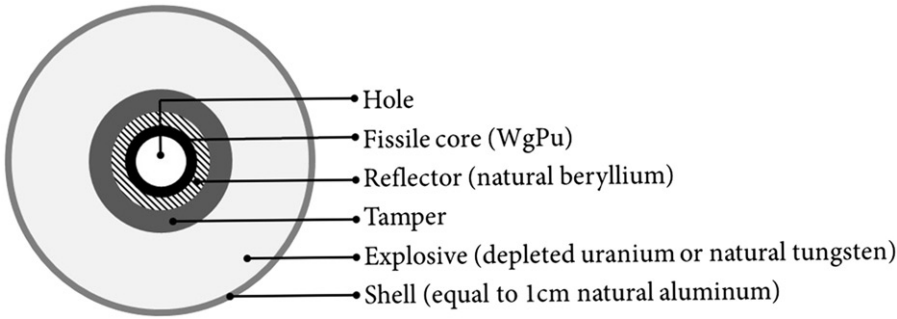


Figure 2. Weapons-grade plutonium warhead model.

the strengths and the branch ratios, the absorption efficiencies can be calibrated. Then, the absorption efficiencies for the characteristic γ rays of other nuclides can be calculated using the energy interpolation calculation in Equation 7:

$$C(E_{\gamma 0}) = C(E_{\gamma 1}) + [C(E_{\gamma 1}) - C(E_{\gamma 2})] \cdot \frac{E_{\gamma 0} - E_{\gamma 1}}{E_{\gamma 1} - E_{\gamma 2}} \quad (7)$$

where $E_{\gamma 0}$ is the energy of the required characteristic γ ray, and $E_{\gamma 1}$ and $E_{\gamma 2}$ are the energies of the characteristic γ rays of nitrogen-14 closest to $E_{\gamma 0}$.

Simulating the passive method

JMCT simulation

JMCT is a Monte Carlo software package for particle transport simulation developed by the Beijing Institute of Applied Physics and Computational Mathematics and Software Center.⁵ JMCT simulates the neutron, photon, and neutron-photon coupling transport, produces three-dimensional models, and operates at high-speeds using parallel processing.⁶ JMCT is widely used to simulate radiation detection, physical designs of reactors, and arms control verification techniques.

WgPu warhead model

The WgPu warhead model used in the simulation was proposed by Steve Fetter in 1990.⁷ It is considered a classic model for studying the physical properties of the warhead. The WgPu warhead model consists of five concentric spheres: a fissile core, a reflector, the tamper, the explosive, and the outer shell (see Figure 2). The warhead takes two forms depending on the tamper materials. Model 1 is depleted uranium, and Model 2 is natural tungsten (see Table 2).

Table 2. Mass and ingredient parameters of structures in a weapons-grade plutonium warhead model.

Structure	Outer radius (cm)	Mass (kg)	Ingredient (parameters)
Hole	4.25	0.0	Vacuum
Fissile core	5.0	4.0	Weapons-grade plutonium (^{238}Pu (0.005%), ^{239}Pu (93.3%), ^{240}Pu (6%), ^{241}Pu (0.44%), ^{242}Pu (0.015%), O(0.22%))
Reflector	7.0	2.0	Natural beryllium
Tamper	10.0	52.0	Model 1: Depleted uranium (^{235}U (0.3%), ^{238}U (99.7%)) Model 2: Natural tungsten
Explosive	20.0	56.0	Explosive (atom number ratio is H:C:N:O = 2:1:2:2)
Shell	21.0	14.0	Natural aluminum

The neutrons in the WgPu warhead have two sources: The fissile material splits spontaneously and produces the fission neutrons whose energy spectrum obeys the Watt distribution approximately:

$$f(E) = C \cdot e^{-E/a} \cdot \sinh\sqrt{bE}$$

$$C = 2 \cdot e^{ab/4} / (a\sqrt{ab\pi}) \quad (8)$$

where E is the neutron energy, and $f(E)$ is the distribution function of the neutron energy spectrum, and a , b are the parameters of the Watt distribution. The alpha particles released by the fissile material have (α, n) reactions with the light nuclides (such as oxygen-18), and the neutrons are produced. The neutron yields of these two sources are shown in Table 3.

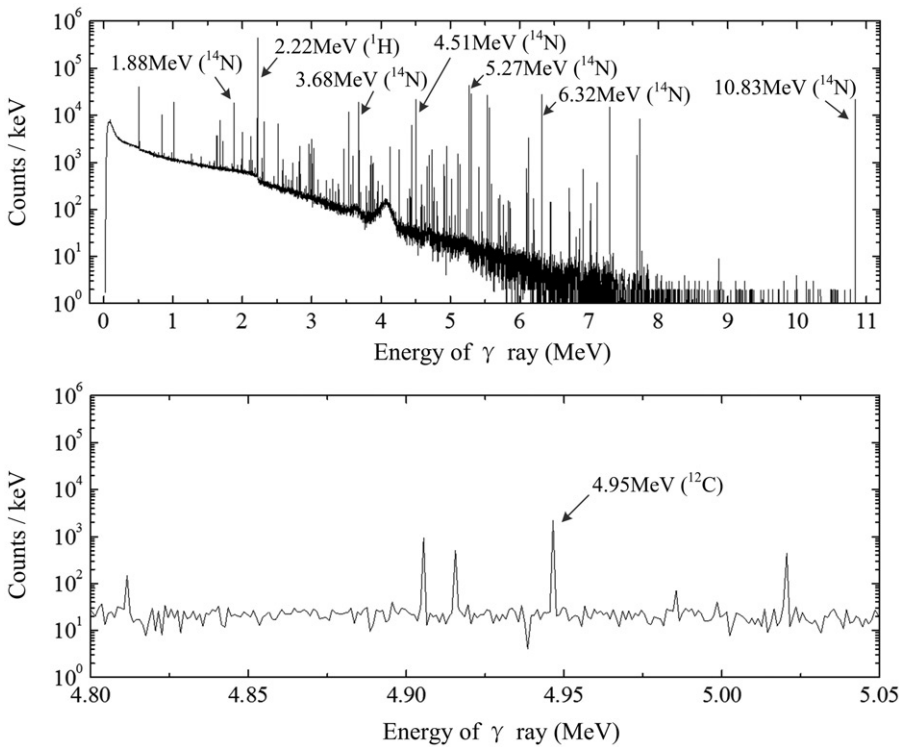
Simulation results

In the simulation, both warhead models produced 10^7 initial neutrons (equivalent to a measurement time of 44.60 seconds and 44.80 seconds for Model 1 and Model 2 respectively). The transport of these initial neutrons in the warhead was simulated, and the energy spectrum of the γ rays emitted from the warhead was modeled. Figure 3 shows the results of Model 1. In Figure 3, the peak positions of the characteristic γ rays of the (n, γ) reactions of hydrogen-1, carbon-12, and nitrogen-14 are illustrated (the energy width of each channel in the energy spectrum is 1 keV).

The event rates of the characteristic γ rays of hydrogen-1, carbon-12, and nitrogen-14 emitted from the warhead is also modeled (see Table 4). Given that the characteristic γ rays emit from the warhead isotropically, and if the high-purity germanium (HPGe) detector with a 65 mm diameter and 60 mm thickness (and an energy resolution of up to $1.80\text{keV}@1.33\text{MeV}$)⁸ is used to detect the characteristic γ rays and is placed 1 meter (m) away from the center of the warhead. When the full-peak counts of the characteristic γ rays achieves a 5% error, the required detection time is shown in Table 4.⁹ From Table 4, the event rate of the

Table 3. Neutron fields of fissile materials with masses of 1 kg.

Material	Nuclide	Neutron yield/neutrons · s ⁻¹			Total neutron yield (neutrons · s ⁻¹)
		(α ,n) reaction	Spontaneous fission	Portion (%)	
Weapons-grade plutonium	Plutonium-238	2.2×10^5	2.5887×10^6	0.005	140.4
	Plutonium-239	630	21.83	93.30	608.2
	Plutonium-240	2300	9.095×10^5	6.0	54708
	Plutonium-241	22	49.43	0.44	0.314
	Plutonium-242	33	1.779×10^6	0.015	266.9
	Oxygen	0	0	0.22	0
Depleted uranium	Uranium-235	0	0.299	0.3	0.001
	Uranium-238	0	13.57	99.7	13.52

**Figure 3.** Energy spectrum of γ rays emitted from the WgPu warhead (Model 1).

characteristic γ rays of carbon-12 is the lowest (the lowest among the characteristic rays shown in Table 1), and their detection time needed to make their counts reach an error of 5% is the longest. Therefore, if the signals of the characteristic γ ray of carbon-12 are adequate, the signals of the characteristic γ rays shown in Table 1 will also be adequate. If one wants to detect the characteristic γ rays of carbon-12 in hydrogen-1 based on the HPGe detector described here, an array of HPGe detectors outside the warhead will improve the detection efficiency of the measurement device. Based on preliminary estimates, an array of 29 HPGe detectors placed on

Table 4. Event rates and detection results of characteristic γ rays of nuclides emitted from weapons-grade plutonium warheads.

Energy of characteristic γ ray (MeV)		2.22 (hydrogen-1)	4.95 (carbon-12)	10.83 (nitrogen-14)
Model 1	Event rate of γ rays emitted from the shell/cps	9.83×10^3	48.6	491
	Full-peak counts of γ rays detected by a single HPGe detector at 1 m/cps	2.10	5.45×10^{-3}	2.20×10^{-2}
	Measurement time to reach 5% error/s	190	7.33×10^4	1.82×10^4
Model 2	Event rate of γ rays emitted from the shell/cps	7.54×10^3	35.2	372
	Full-peak counts of γ rays detected by a single HPGe detector at 1 m/cps	1.61	3.94×10^{-3}	1.67×10^{-2}
	Measurement time to reach 5% error/s	248	1.01×10^5	2.40×10^4

the spherical surface 1 m from the center of the warhead can fulfill the demand.

Background interference may confound detection. Assuming the warhead is in a large building with a concrete floor, it can be assumed that a source of interference is characteristic γ rays produced by the concrete under the warhead. A simulation was carried out to calculate this background interference. In the simulation, the WgPu warhead and the HPGe detector are placed 1 m above the floor; the distance between the center of the warhead and the detector is 1 m; the floor has a thickness of 1 m and consists of hydrogen, oxygen, sodium, aluminum, silicon, and iron (their atom percentages are 14.30%, 78.60%, 1.90%, 4.50%, 0.30%, and 0.40%, respectively). The results show that, the intensity of the 2.22 MeV characteristic γ rays of hydrogen-1 entering the detector from the floor is about 0.3 cps (counts per second), while that from the WgPu warhead is about 10.3 cps. Therefore, the influence of the background on the counts of the characteristic γ rays of hydrogen-1 is about 3%. Taking account of the 3%, the counts of the 2.22 MeV characteristic γ rays of hydrogen-1 detected by a single HPGe detector should reach 412, versus 400 without the background effect to reach a count error of 5%. A lead shield between the detector and the floor would effectively suppress the background.

By counting the peak counts of the series of the characteristic γ rays of nitrogen-14 (Table 1) emitted from the warhead and calculating the ratios between the peak counts and the branch ratios of the characteristic γ rays, the absorption efficiencies of the warhead to γ rays can be calibrated (normalized to 10.83 MeV γ ray) (Figure 4).

Next, by counting the peak counts of the characteristic γ rays of hydrogen-1, carbon-12, nitrogen-14 (Table 1) emitted from the warhead,

and combining the calculations, the element number ratios of the explosive in the warhead, such as $[H]/[N]$ and $[C]/[N]$, can be calculated (Table 5). It also can be seen in Table 5 that the errors of the reconstructed values of $[H]/[N]$ and $[C]/[N]$ do not exceed 5%.

Since the passive method proposed by this paper has high reconstruction precision of the element number ratios (include $[H]/[N]$ and $[C]/[N]$) of the explosive in the warhead (Table 5), this method can identify the existence of an explosive warhead before it is dismantled by analyzing whether $[H]/[N]$ and $[C]/[N]$ of the materials in the warhead fit the element constitution of the explosive. Table 6 shows the reconstructed element number

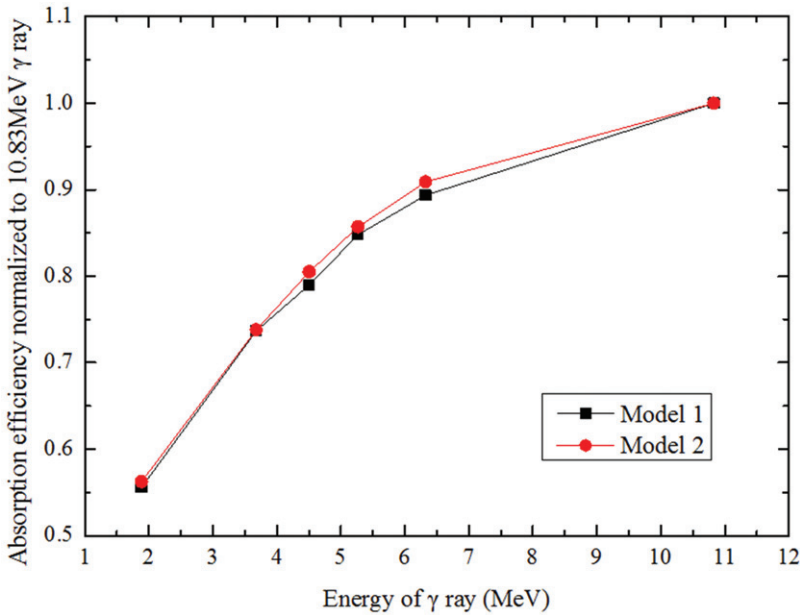


Figure 4. Absorption efficiency of weapons-grade plutonium warheads to γ rays.

Table 5. Reconstruction results of element number ratios of explosive.

Element number ratio	Value	Reconstruction values	
		Model 1	Model 2
$[H]/[N]$	1.00	1.01	1.02
$[C]/[N]$	0.5	0.525	0.495

Table 6. Reconstruction results of element number ratios of TNT, PETN and Tetryl in weapons-grade plutonium warheads using Model 1.

Explosive	Molecular formula	$[H]/[N]$		$[C]/[N]$	
		Actual value	Reconstructed value	Actual value	Reconstructed value
TNT	$C_7H_5N_3O_6$	1.67	1.68	2.33	2.37
PETN	$C_5H_8N_4O_{12}$	2.00	2.02	1.25	1.27
Tetryl	$C_7H_5N_5O_8$	1.00	0.988	1.40	1.44

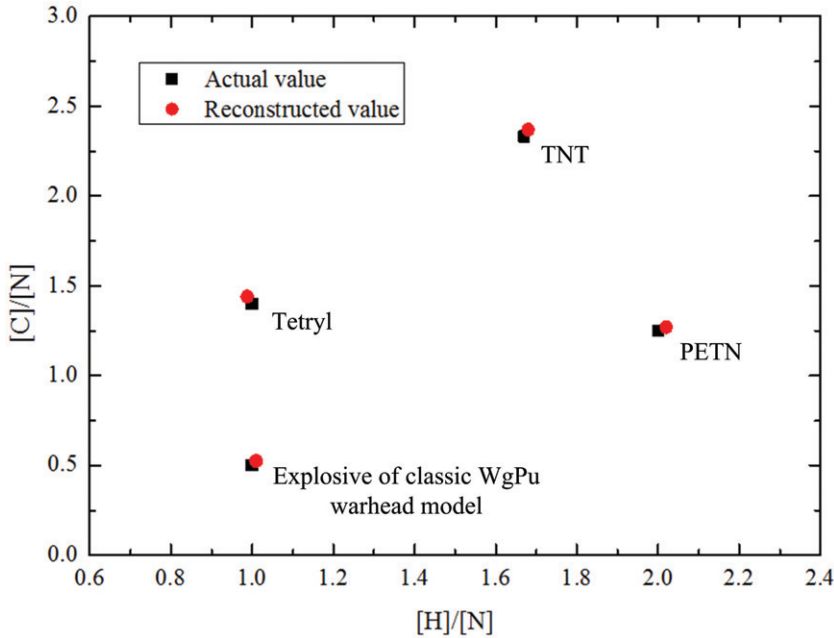


Figure 5. Reconstruction results of element number ratios of several different explosives in weapons-grade plutonium warheads (taking Model 1 for example).

ratios of three different types (TNT, PETN, and tetryl) of the explosives in the warheads (taking Model 1 for example) based on the passive method. It is found that TNT, PETN, and tetryl can be identified based on the reconstruction results of their $[H]/[N]$ and $[C]/[N]$ (Figure 5). Therefore, in disarmament verification, this method contributes to judging whether the pre-dismantled warhead is included under the treaty.

To justify that the simulation results of the explosive element analysis above are not configuration-specific, a simulation based on a varied WgPu warhead model was carried out. In the varied WgPu warhead model, there is no beryllium layer, and the aluminum shell is varied to an iron shell. Per the simulation result, the reconstructed $[H]/[N]$ and $[C]/[N]$ are 1.010 and 0.543 respectively. These values are in agreement with the actual values, which confirms that the simulation results stated above are not configuration-specific.

Conclusion

This paper proposes a passive detection method of the explosive in the warhead based on the neutron analysis techniques. The simulation based on the JMCT software shows that, by establishing an array of HPGe detectors, the elements of hydrogen, carbon, and nitrogen of the explosive in the warhead can be detected in hydrogen-1 (at an error of 5%). Finally, based

on the simulation results, the reconstructed element number ratios of the explosive in the warhead are in agreement with the actual values. At these levels of precision, the passive method can determine whether an explosive is present and distinguish between a WgPu warhead and a fake one without explosives. In addition, the passive method can distinguish the types of the explosives in the WgPu warheads. This capability can improve the reliability and effectiveness of nuclear disarmament verification to prevent a verified party from circumventing the verification process.

Notes and References

1. C. T. Olinger, W. D. Stanbro, R. G. Johnstan et al., “Technical Challenges for Dismantlement Verification,” LA-UR-97-2812, Los Alamos National Laboratory (1997); D. W. Macathur, D. K. Hauck, M. Smith, “Confirmation of Nuclear Treaty Limited Items – Pre-Dismantlement vs. Post-Dismantlement,” LA-UR-13-23004, Los Alamos National Laboratory (2013); C. T. Olinger, M. Frankle, M. W. Honson et al., “Measurement Approaches to Support Future Warhead Arms Control Transparency,” LA-UR-98-3115, Los Alamos National Laboratory (1998); D. K. Hauck, D. W. Macathur, “Benefits of a ‘Presence of Fissile Material’ Attribute for Warhead Confirmation in Treaty Verification,” LA-UR-13-25330, Los Alamos National Laboratory (2013); M. Kutt, S. Philippe, B. Barak et al., “Authenticating Nuclear Warheads with High Confidence,” Institute of Nuclear Materials Management, 55th Annual Meeting of the Institute of Nuclear Materials Management, Atlanta, Georgia, USA, 20–24 July 2014, Vol. 1. (Curran: Red Hook, NY, 2014); R. Voznyuk, M. Charles, A. Renlund et al., “High Explosive Detection and Destruction Technology Applications for Warhead Dismantlement Transparency,” Sand 2000-1533C, Sandia National Laboratory (2000).
2. Z. D. Whetstone, K. J. Kearfott, “A review of conventional explosives detection using active neutron interrogation,” *Journal of Radioanalytical and Nuclear Chemistry* 301 (2014): 629–639. doi: 10.1007/s10967-014-3260-3265; Wen Ding, Yuling Dou, Guobao Wang et al., “Review on detection technology for explosives,” *Explosive Materials* 40, 5, 33–37: (2011). (in Chinese); S. K. Sharma, S. Jakhar, R. Shukla et al., “Explosive detection system using pulsed 14MeV neutron source,” *Fusion Engineering and Design* 85 (2010): 1562–1564. doi: 10.1016/j.fusengdes.2010.04.044; P. Shea, T. Gozani, H. Bozorgmanesh, “A TNA explosives-detection system in airline baggage,” *Nuclear Instruments and Methods in Physics Research, Section A*, (1990): 299, 444–448. doi: 10.1016/0168-9002(90)90822-N.
3. ENDF: Evaluated Nuclear Data File [EB/OL]. [2016-11-09]. <https://www-nds.iaea.org/exfor/endl.htm>.
4. Ibid
5. Beijing Institute of Applied Physics and Computational Mathematics and Software Center, High Performance Numerical Simulation, China Academy of Engineering Physics, <http://www.iapcm.ac.cn/website/js/index.html?siteid=8a8a83c941edc0330141edc74b450014>
6. Gang LI, Baoyin Zhang, Li Deng et al., “Development of Monte Carlo particle transport code JMCT,” *High Power Laser and Particle Beams* 25 (2013): 158–162. (in Chinese); Li Deng, Gang LI, Baoyin Zhang et al., “Simulation of Full-core pin-by-

- pin Model by JMCT Monte Carlo Neutron-photon Transport Code,” *Atomic Energy Science and Technology* 48 (2014): 1061–1066. (in Chinese)
7. S. Fetter, “Detecting Nuclear Warheads,” *Science & Global Security* 1 (1990): 225–302. doi: 10.1080/08929889008426333; Jun Wu, “Numerical Simulation Study of Nuclear Warhead Detection Techniques,” Mianyang: China Academy of Engineering Physics (2003). (in Chinese)
 8. Produced by ORTEC Advanced Measurement Technology, <https://www.ortec-online.com/products/radiation-detectors/germanium-hpge-radiation-detectors>
 9. The full-peak detection efficiencies of the detector are 20.3%, 10.6% and 4.25% for the characteristic γ rays with the energy of 2.22MeV, 4.95MeV and 10.83MeV respectively.